

Spin-1/2 frustrated antiferromagnet on a spatially anisotropic square lattice: contribution of exact diagonalizations.

P. Sindzingre

Laboratoire de Physique Théorique des Liquides-UMR 7600 of CNRS, Université Pierre et Marie Curie, case 121, 4 place Jussieu, 75252 Paris Cedex, France
E-mail: phsi@lptl.jussieu.fr

(October 29, 2018)

The phase diagram of a spin-1/2 $J - J' - J_2$ model is investigated by means of exact diagonalizations on finite samples. This model is a generalization of the $J_1 - J_2$ model on the square lattice with two different nearest-neighbor couplings J, J' and may be also viewed as an array of coupled Heisenberg chains. The results suggest that the resonating valence bond state predicted by Nersisyan and Tsvetlik [Phys. Rev. B **67**, 024422 (2003)] for $J_2 = 0.5J' \ll J$ is realized and extends beyond the limit of small interchain coupling along a curve nearly coincident with the line where the energy per spin is maximum. This line is likely bordered on both sides by a columnar dimer long range order. This columnar order could extend for $J' \rightarrow J$ which correspond to the $J_1 - J_2$ model.

PACS numbers: 75.10.Jm; 75.50.Ee; 75.40.-s

I. INTRODUCTION

The interplay between frustration and quantum fluctuations in antiferromagnetic (AF) spin-1/2 systems in two dimensions (D) has attracted much experimental and theoretical attention in past years. In particular, many studies have been devoted to identify the possible phases which may appear at $T = 0$ after the destabilization of a collinear AF Néel phase by quantum fluctuations when increasing frustration in $SU(2)$ invariant spin models. Large- N approaches predict then a valence bond crystal (VBC) phase, with long range order (LRO) of singlet entities (dimers, plaquettes of resonating dimers...) and thus breaking translational symmetry and/or others space symmetries, if the transition out of the Néel phase is continuous [1–3]. Numerical results obtained from exact diagonalization (ED) studies support this prediction for several models: the $J_1 - J_2 - J_3$ model on the honeycomb lattice [4] and some models where the spins sit on a square lattice such as the crossed chain model [5,6] and the quadrumerized Shastry-Sutherland model [7].

Yet, for the much studied $J_1 - J_2$ model on the square lattice with a next-nearest-neighbor frustrating coupling J_2 in addition to the nearest-neighbor coupling J_1 (see Fig. 1 where the $J_1 - J_2$ model corresponds to $J' = J = J_1$), the validity of this scenario remain unclear [8–17]. Its classical ground-state has (π, π) Néel LRO for $J_2 < 0.5J_1$ and is the degenerate manifold corresponding to two decoupled Néel states on interpenetrating square lattices for $J_2 > 0.5J_1$. There is a large consensus that (π, π)

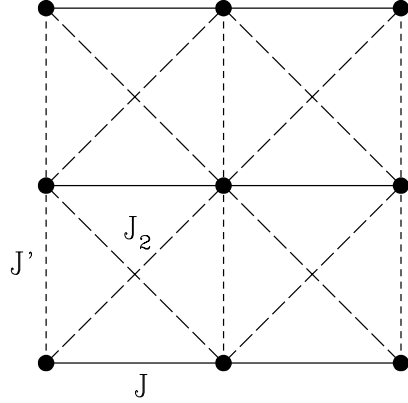


FIG. 1. Exchange interaction pattern in the $J - J' - J_2$ model. The spins sit at the vertices shown by bullets, the coupling constant is J between nearest-neighbor pairs on horizontal bonds (full lines), J' on vertical bonds (short dashed lines) and J_2 on the diagonal bonds (long dashed lines). The $J_1 - J_2$ model corresponds to $J' = J = J_1$.

Néel LRO (see Fig. 2) survives to quantum fluctuations for $J_2 \lesssim 0.4J_1$ and quantum fluctuations select either a $(\pi, 0)$ or a $(0, \pi)$ Néel state in the manifold of classical ground-states for $J_2 \gtrsim 0.65J_1$, whereas, in the intermediate range $0.4J_1 \lesssim J_2 \lesssim 0.65J_1$ between these two gapless states, there is a phase without Néel LRO gapped to spin excitations. The transition out of the (π, π) Néel phase is second order while the transition out of the $(\pi, 0)$ Néel phase has been predicted to be of first order [10] but may be close to second order [14].

Whether this intermediate phase has VBC LRO or is some resonating valence bond (RVB) phase which do not break any space symmetries, i.e. a spin-liquid, is debated. Earliest investigations, from ED calculations on samples up to $N = 36$ spins, have shown enhanced columnar dimer-dimer correlations in this intermediate region, but the finite-size scaling of the order parameter for the columnar VBC LRO of dimers, shown in Fig. 3(a), were not conclusive [8,9]. Dimer series expansions, however, were in favor of VBC LRO: earliest studies favored columnar LRO [10,11] while latter calculations have lead to propose the occurrence of two different

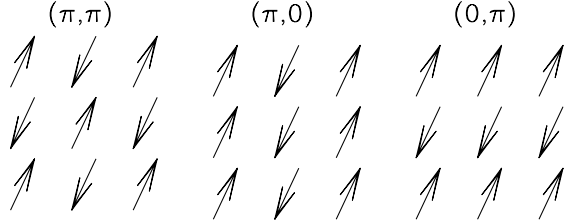


FIG. 2. Spins orders in the classical (π, π) , $(\pi, 0)$ and $(0, \pi)$ Néel states.

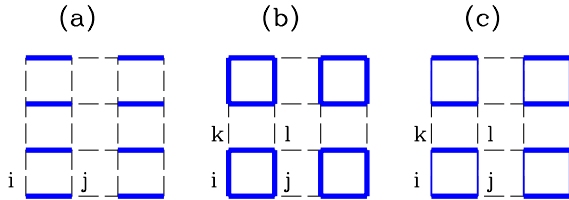


FIG. 3. Patterns of VBC orders proposed for $J_1 - J_2$ model: (a) columnar dimer, (b) plaquette, (c) columnar dimer with plaquette type modulation. Full lines connect spins bound into singlet: two spins in (a), four spins in (b) and (c). In (b) the strength of spin-spin correlations on vertical and horizontal links of a plaquette i, j, k, l are the same but differs in (c). There are four degenerate ground-states for orders (a), (b) and eight for the order (c) in the $J_1 - J_2$ model. These are obtained by one step translations in the horizontal and vertical directions and/or a $\pi/2$ rotation around a lattice site.

VBC phases: the columnar dimer phase for $J_2/J_1 \lesssim 0.5$ and a columnar dimer phase with plaquette type modulation, as shown in Fig. 3(c), for $0.5 \gtrsim J_2/J_1$, separated by a second order transition [14]. On the other hand, studies based on the Green function Monte Carlo method, for systems of sizes larger than those which may be investigated by ED calculations, first favored either a plaquette LRO [12], as shown in Fig. 3(b), or a columnar dimer LRO with plaquette type modulation [13], similar to one of Ref [14], for $J_2/J_1 = 0.5$. Besides, it was concluded in Ref [12] that the finite size scaling of the susceptibility to columnar dimer LRO from both Monte Carlo and ED calculations would exclude columnar dimer LRO at $J_2 = 0.5J_1$. However, latter calculations [15], by the same group which favored the plaquette LRO [12], have lead to conclude in favor of the occurrence of a spin-liquid phase for $0.4J_1 \lesssim J_2 \lesssim 0.5J_1$ whereas it was pointed out that the occurrence of the plaquette LRO will be unlikely in view of the spatial symmetries of the low lying singlets in the ED spectra. In their latest study these authors suggest either a spin-liquid or, possibly, the columnar state but with a weak order parameter [17] Yet, as the Monte Carlo calculations and the series expansions start

from some trial state which may bias the results and involve approximations which are not fully under control, while ED calculations which were performed on samples having different lattice symmetries and display irregular finite size scaling, the nature of the ground-state in the intermediate region remain an open question.

In this paper, motivated by a recent paper of Nersisyan and Tsvelik [18], referred as (NT) in the following, we attempt to shed light on this issue from ED calculations on a spatially anisotropic version of the $J_1 - J_2$ model with two different nearest neighbor couplings. The Hamiltonian of this $J - J' - J_2$ model (named the confederate flag model by NT) reads:

$$\mathcal{H} = \sum_m^M \sum_l^L [J \mathbf{S}_{l,m} \cdot \mathbf{S}_{l+1,m} + J' \mathbf{S}_{l,m} \cdot \mathbf{S}_{l,m+1} + J_2 (\mathbf{S}_{l,m} \cdot \mathbf{S}_{l+1,m+1} + \mathbf{S}_{l,m} \cdot \mathbf{S}_{l+1,m-1})] \quad (1.1)$$

which may also be viewed as an array of M spin chains of length L , if $J' < J$. The exchange J (see Fig. 1) couples first-neighbor (horizontal) pairs of spins along the chains, exchange J' first-neighbor spins in the (vertical) transverse direction and exchange J_2 second-neighbor pairs on the diagonals of the square plaquettes. All exchanges are assumed positive, describing AF couplings. For $J' = J$ one recovers the $J_1 - J_2$ model. Mostly interested with the limit $M, L \rightarrow \infty$, we shall also focus on the case $J' \leq J$.

The classical ground-state of the $J - J' - J_2$ model is rather similar to the one of the $J_1 - J_2$ model. When $J' < J$, one has (π, π) Néel LRO if $J_2 < 0.5J'$, $(\pi, 0)$ Néel LRO if $J_2 > 0.5J'$ and the (horizontal) J chains are decoupled if $J_2 = 0.5J'$. For $J' > J$, one has (π, π) Néel LRO if $J_2 < 0.5J$, $(0, \pi)$ Néel LRO if $J_2 > 0.5J$ whereas the (vertical) J' chains are decoupled if $J_2 = 0.5J$.

This Hamiltonian has been much studied in past years for a finite number of chains, the so-called M -leg ladders, generally in the case of open boundary conditions in the transverse direction (for $M > 2$ since if $M = 2$ open and periodic boundary conditions are equivalent).

Numerical studies [27–29] based on the density matrix renormalization group (DMRG) method or Monte Carlo approaches have shown that the M -leg unfrustrated ladders ($J_2 = 0$) display a behavior analogous to a $M/2$ -spin chain [26], being fully gapped if M is even and gapless if M is odd. So (π, π) Néel LRO only occurs in the limit $M \rightarrow \infty$.

The effect of frustration has been especially investigated theoretically and numerically for the 2-leg ladder (see Ref [21–24] and references therein). These studies have concluded that one has two phases separated by a transition line which has been found to coincide with the line of maximum frustration where the energy per spin reaches its maximum, noted $J_2^m(J')$ in the following for all values of the number of chains. This line starts as $J_2^m(J') \sim 0.5J'$ for $J' \rightarrow 0$ and bend slightly with increasing J' so that $J_2^m(J') \sim 0.6$ at $J' = 1$ [21,22] (as the dashed line in Fig. 4). If $J_2 > J_2^m(J')$ one has the ‘Haldane phase’, where the two spins on a rung tend to

be in a triplet state, so named as it contains the point $J_2 = J, J' = 0$ whose low-energy spectrum is similar to that of a spin-1 Heisenberg chain. If $J_2 < J_2^m(J')$ on has the so called 'singlet phase', so called as it contains the case $J' \gg J$ with $J_2 = 0$, where the ground-state consists of singlets on each rung. As shown by White [31] the 'singlet phase' is also an Haldane phase with diagonally situated next-nearest neighbor spins coupling to form an effective $S = 1$. Both phases have a topological order, breaking a hidden $Z_2 \times Z_2$ symmetry, which can be measured by non-local 'string order' parameters, similar to the string order parameter of the $S = 1$ Heisenberg chain. The two phases are fully gapped like the $S = 1$ chain [26], and have a non degenerate singlet ground-state. These ground-states become degenerate on the transition line $J_2^m(J')$. The nature of the transition has been debated. In a DMRG study [22] it was predicted that the transition line would be gapless for J_2 lower than $\approx 0.287J$. But more recent DMRG calculations [23] have concluded that a gap subsists between the two-fold degenerate ground-state and the excited states for all $J_2 > 0$. So the transition is 1th order on the whole line $J_2^m(J')$ in agreement with bosonization results in the limit of vanishing interchain coupling [24]. The elementary excitations then consist of gapped deconfined spin-1/2 spinons which may be viewed as kinks interpolating between the two ground-states [24]. Note that these results imply that the classical behavior of independent chains on the line $J_2 = 0.5J'$ is then destabilized by quantum fluctuations. The single Heisenberg chain is gapless. The spectrum of two independent chains too. The existence of a finite gap excludes such a behavior.

A DMRG study of the three-leg frustrated ladder with open boundary conditions in the transverse direction [25] has shown that this system exhibit two phases separated by a transition line also coincident with the line of maximum frustration $J_2^m(J')$ and which is a curve quasi identical to the one found for the 2-leg ladders. The phases are analogous to those of the 2-leg ladders. The small J_2 phase, which is the phase of the unfrustrated ladder, show a tendency of the three spins on a vertical line to pair in a state of minimum spin whereas they tend to pair in a state of maximum spin in the large J_2 phase, which is equivalent to the spin-3/2 chain. On the transition line a bosonization study at weak interchain coupling [32] has predicted that the ground-state is a chiral spin-liquid.

Recently NT, using an approach based on the bosonization method, investigated the crossover from finite M to $M \rightarrow \infty$ in the $J - J' - J_2$ model on the line $J_2 = 0.5J'$, in the limit of small interchain coupling ($J', J_2 \ll J$) and predicted that the classical behavior of independent chains is unstable to a special RVB (spin-liquid) state which may be a realization of the chiral π -flux RVB state [18–20]. Its ground-state has a 2^{M-1} degeneracy, for M even and transverse periodic boundary conditions, associated to the breaking of a local Z_2 symmetry, present in the bosonised version of the model, corresponding to the invariance under

independent translations by one lattice spacing along individual chains. Each ground-state may be characterized by different values of a set of non-local order parameters. These non-local order parameters correlate spins on two adjacent chains whereas different pairs of chains are uncorrelated. The elementary excitations consist of deconfined spin-1/2 spinons interpolating between different ground-states. These excitations are either gapless, as predicted for some values of the number of chains, such as $M = 4, 6, 12$, or gapped, as for the 2-leg ladder ($M = 2$).

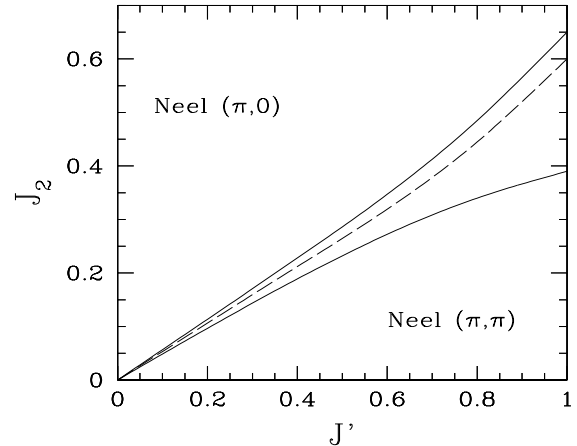


FIG. 4. Proposed phase diagram of the $J - J' - J_2$ model for $L \rightarrow \infty$ and $M \rightarrow \infty$ ($J = 1$). The solid lines indicate the approximate location of the boundaries of the (π, π) and $(\pi, 0)$ Néel phases, noted $J_2^{c1}(J')$ and $J_2^{c2}(J')$ respectively. The dashed line in the intermediate region between the Néel phases is the approximate location of the maxima $J_2^m(J')$ of the energy per spin e_0 along which the present ED results suggest that the RVB state predicted by NT may be realized up to large values of J' . In the intermediate region, outside the curve J_2^m , the ground-state is predicted to display columnar dimer order. The Néel phases only appear for both $L, M \rightarrow \infty$. For finite M and $L \rightarrow \infty$ one has gapped phases. The position of the curve $J_2^m(J')$ is quasi-independent of the number M of chains down to $M = 2$, which correspond to the 2-leg ladder.

Two questions then arise. First, does the state predicted by NT extends outside the range of small interchain coupling. Second, what is the nature of the behavior in its vicinity, in particular for the case of an infinite number of chains. Below we report results of ED calculations of $N = M \times L$ spins for $N \leq 36$ to shed light on these questions and more generally the phase diagram of the $J - J' - J_2$ model. We shall consider only the case of an even number of chains. The ED calculations have been carried out on samples of $N = M \times L$ spins in M chains of lengths L with periodic boundary conditions both along and perpendicular to the chains: samples of 4 chains with $N = 16, 24, 32, 36$ spins and 6 chains with

$N = 24, 36$ spins. Additional calculations were also performed for the $M = 2$ ladder for $N \leq 32$ in order to compare with the $M = 4, 6$ results. Contrary to the samples considered in previous ED calculations for the $J_1 - J_2$ model, all samples have translation vectors parallel to the basis vectors of the square lattice which leads to a regular evolution of the properties with increasing L and M .

Examination of the ED spectra indicates that the model will display two Néel phases, with magnetic wave-vectors (π, π) and $(\pi, 0)$, separated by a magnetically disordered intermediate region, in the limit $N \rightarrow \infty$ with both $L \rightarrow \infty$ and $M \rightarrow \infty$, as shown in Fig. 4. At variance with a study based on the DRMG method [33], which appeared very recently on a preprint server, our results provide indications that the classical behavior of independent chain is destabilized by quantum fluctuations and the RVB state of NT may occur along a curve coincident with the line of maximum frustration $J_2^m(J')$, located in this intermediate region, up to large interchain coupling. They also indicate that the intermediate region of the $M \rightarrow \infty$ phase diagram (see Fig. 4), on both sides of this line, has columnar VBC LRO, which may extend up to $J' \rightarrow J$ and could already appear for M even ≥ 4 .

In Sec.II we describe the evolution of the energy per spin vs J_2 and J' and the location of the curve $J_2^m(J')$. The properties of the model in the regions of (π, π) Néel LRO, $(\pi, 0)$ Néel LRO and in the intermediate region are presented in Sec. III, IV and V, respectively. Sec. VI gives a summary of our results and discuss briefly the possible behavior of the model for ferromagnetic J_2 and J' .

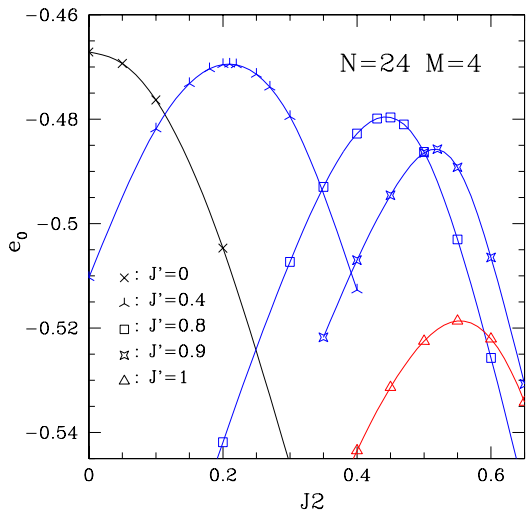


FIG. 5. Ground-state energies per spin $e_0 = E_0/N$ vs J_2 for the $N = 24$ sample with $M = 4$ (4 chains). The lines are guides to the eyes.

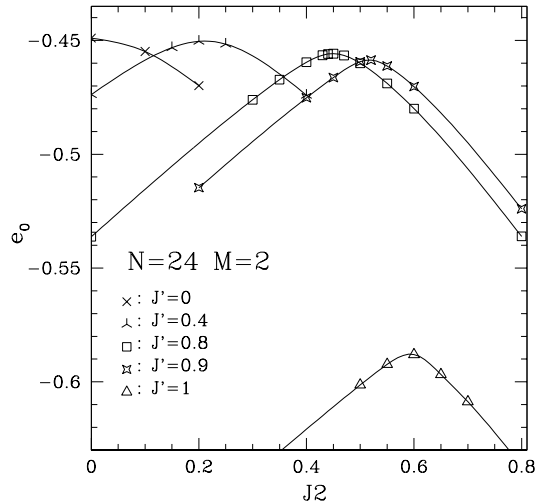


FIG. 6. Same as Fig. 5 for the $N = 24$ sample with $M = 2$ (2-leg ladder).

II. ENERGY RESULTS

The ground-state energies per spin $e_0 = E_0/N$ are plotted, as a function of J_2 , for different values of $J' \leq 1$ ($J = 1$ in the following) for the $M = 4$ chains, $N = 24$, sample in Fig. 5. For comparison, the results for the $N = 24$ 2-leg ladders are indicated in Fig. 6. Fig. 7, displays e_0 vs J_2 at $J' = 0.8$ for the different $M = 4$ and $M = 6$ samples. As shown in Fig. 5 and Fig. 7, the point of "maximum frustration" where e_0 reaches its maximum, $J_2^m(J')$ occurs for a value of J_2 slightly larger than $0.5J'$, as found for the two and three-leg ladders [21,22,25].

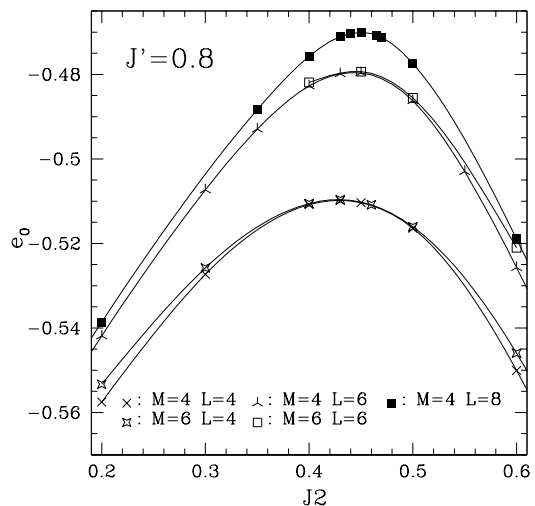


FIG. 7. Ground-state energies per spin $e_0 = E_0/N$ vs J_2 at $J' = 0.8$ for different samples of M chains of lengths L .

As shown in Fig. 7, J_2^m slightly increases with L , but is nearly independent of the number M of chains. This indicates that the $L \rightarrow \infty$ curves $J_2^m(J')$ will be quasi-independent of M , as previously conjectured from a comparison of the results for the two and three-leg ladders [25]. The maxima of e_0 (for a given sample) decrease with increasing J' but remain rather close to the value for decoupled chains at $J' = 0$ at least if $J' \leq 0.9$.

In Fig. 5 and Fig. 6 one sees, in the range $0.9 < J' < 1$ a drop of e_0 at J_2^m from a value close to the one for decoupled J chains of lengths L to a value closer to the one for independent J' chains of lengths M . This corresponds to the crossover to the situation at $J' \gtrsim 1$ where the finite samples $M \times L$ are best viewed as L coupled chains of finite lengths M .

III. (π, π) NÉEL LONG RANGE ORDER

Increasing J_2 from zero at given J' (≤ 1), one finds a range of parameters, which extends to a value we note $J_2^{c1}(J')$, slightly smaller than $0.5J'$ (and thus $< J_2^m(J')$), where the spectra exhibit the features at finite size specific of a system displaying collinear (π, π) Néel LRO in the limit $N \rightarrow \infty$ with both $L \rightarrow \infty$ and $M \rightarrow \infty$. The Néel order breaks $SU(2)$ and lattice spacial symmetries. Evidence of Néel LRO in the spectra is the presence of lowest eigenlevels in each spin S sector which form a set of states with energies $E(S) - E_0 \sim S(S+1)/N$ for $L \rightarrow \infty$ and $M \rightarrow \infty$, the so-called quasi degenerated joint states (QDJS) [34,5] as shown in Fig. 8. These QDJS are well separated, at finite size, from the others lowest excited states (magnons) and collapse on the ground-state faster with N than the magnons, enabling the breaking of $SU(2)$ and lattice spacial symmetries. For collinear LRO there is one QDJS for each S value. The QDJS specific of (π, π) Néel LRO consist of a state belonging to an irreducible representation (IR) with wave-vector $\mathbf{k} = 0$ if S is even or $\mathbf{k} = (\pi, \pi)$ if S is odd, both even in a spatial $R(\pi)$ rotation around a site and in the reflexion σ with respect to a J chain.

The approach of ED calculations does not allow an accurate location of boundary of the Néel phase since it is limited to small samples. Nevertheless the extension of the Néel phase can be approximatively estimated from ED calculations by monitoring the range of values of J_2 for which the QDJS remain well defined in the spectrum [5]. This gives $J_2^{c1}(J' = 1) \approx 0.4$ for the $J_1 - J_2$ model, $J_2^{c1}(J' = 0.8) \approx 0.35$. $J_2^{c1}(J')$ moves steadily closer to the line $J_2 = 0.5J'$ as J' decreases. Besides, since quantum Monte Carlo calculations on the unfrustrated line of the phase diagram ($J_2 = 0$) have indicated that (π, π) LRO appear as soon as $J' > 0$ for $M \rightarrow \infty$ [30], Néel LRO extend down to the point $J' = 0, J_2 = 0$. Thus the curve $J_2^{c1}(J')$ is tangent to the line $J_2 = 0.5J'$ for $J' \rightarrow 0$, moving away from this line as J' increases from zero, and is located below the line,

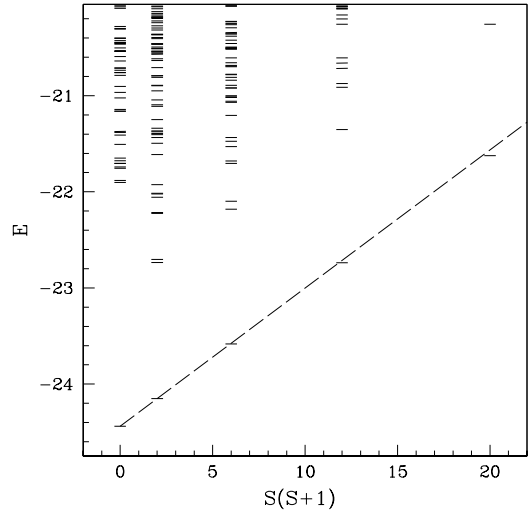


FIG. 8. Spectrum at $J' = 1$ and $J_2 = 0$ vs $S(S+1)$ for $N = 36$. The QDJS characteristic of collinear Néel LRO at the bottom of each S sector are well aligned (dashed line) and clearly separated from the other lowest excitations (see text).

as shown in Fig. 4.

It is to be emphasized that Néel LRO appear only for both $M \rightarrow \infty$ and $L \rightarrow \infty$. There is no Néel LRO for a finite number M of chains. Indeed, as mentioned above, systems which consist of a finite number M of $S = 1/2$ Heisenberg chains are known to acquire a gap upon shifting a transverse coupling J' if M is even, behaving analogously to a spin $S = M/2$ chain, so these systems are in a Haldane phase [27–30].

The typical evolution of the spin-gap Δ^1 with M and L is illustrated in Fig. 9 where values of the Δ^1 are plotted vs $1/N$ for $N = 16, 24, 32$ samples of $M = 4$ chains and the $N = 24, 36$ samples of $M = 6$ chains at $J' = 0.8$ and $J_2 = 0$. The evolution for $M = 4$ of Δ^1 vs $1/N \sim 1/L$ shows a small but noticeable upward curvature as found previously for the 2-leg and 4-leg ladders (see Fig.1 of Ref. [27]). As found in studies of the 2,4,6 legs ladders, one may assume that the gap decreases monotonically as $1/L$ decreases with a curvature that remains positive and vary only smoothly. To estimate a lower bound on $\Delta^1(L \rightarrow \infty)$ we use a linear extrapolation vs $1/L$, beyond $N > 32$ of a spline fit to the $M = 4$ three values of Δ^1 (dashed line in Fig. 9). This leads to a lower bound of Δ^1 for $L \rightarrow \infty \sim 0.09$. This lower bound indicates that $\Delta^1(L \rightarrow \infty)$ remains finite. Due to the neglect of the curvature beyond $N > 32$ the gap is slightly underestimated. The true value of Δ^1 for $L \rightarrow \infty$ for $M = 4$ is likely somewhat closer to the value (~ 0.14) estimated for the 4-leg ladder with open boundary conditions in the transverse direction [28]. For $M = 6$, the present data, limited to the two values for $L = 4, 6$, show that $\Delta^1(L \rightarrow \infty)$ decreases with increasing M , and remain finite if $M = 6$. Its value for the 6-leg ladder is ~ 0.04 [28]

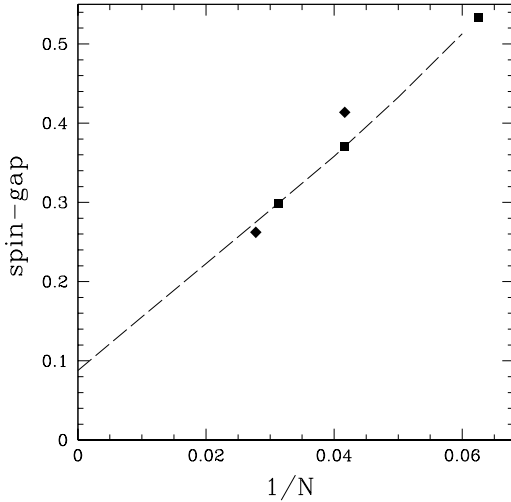


FIG. 9. Spin-gaps at $J' = 0.8$ and $J_2 = 0$ vs $1/N$ for $N = 16, 24, 32$ samples of $M = 4$ chains (squares) and the $N = 24, 36$ samples of $M = 6$ chains (diamonds). The dashed line is a spline fit to the $M = 4$ values for $N \leq 32$ followed by linear extrapolation for $N > 32$.

if $J' = 0.8$. The present data show that the gap is very small but do not allow an accurate estimation of a gap of this order of magnitude.

The evolution of the spin-gap with $N \rightarrow \infty$ for $M = L$ is different than for fixed M and $L \rightarrow \infty$. For $M = L$, where $\Delta^1 \rightarrow 0$ for $N \rightarrow \infty$, the $N = 16, 36$ values in Fig. 9 indicates an evolution of the spin-gap in the case $M = L$ that decreases with a negative curvature vs $1/N$ as usually found in systems with Néel LRO [35].

IV. $(\pi, 0)$ NÉEL LONG RANGE ORDER

For J_2 larger than a value J_2^{c2} , larger but very close to J_2^m , one similarly recognizes in the spectra, the features specific of collinear Néel LRO with a wave vector $(\pi, 0)$ or $(0, \pi)$ depending on value of J'/J .

If $J' = J = 1$ and $M = L$ these two Néel orders are degenerate. The QDJS then include two states for each value of S : two with $\mathbf{k} = 0$ if S is even and two with $\mathbf{k} = (\pi, 0)$ and $\mathbf{k} = (0, \pi)$ if S is odd, all even in $R(\pi)$ and σ .

The degeneracy is lifted if $J' \neq J$. For $J' < J$ and in the thermodynamic limit $M = L \rightarrow \infty$ the $(\pi, 0)$ LRO is favored whereas this would be $(0, \pi)$ LRO for $J' > J$. The QDJS of $(\pi, 0)$ LRO are observed as the lowest states of the spectra as soon as $J' < J$ for $M = L$. They include only one state for each value of S : a state with $\mathbf{k} = 0$ if S is even and a state with $\mathbf{k} = (\pi, 0)$ if S is odd, both even in $R(\pi)$ and σ .

Note, however, that at finite size, for an aspect ratio $M/L < 1$ of the samples, quantum fluctuations, which

favor an antiferromagnetic alignment of the spins in the shortest direction, lead to spectra characteristic of $(0, \pi)$ LRO even for $J' < J$ as $J' \approx J$. The transition between the two kind of spectra then occurs in the range of values of J' where e_0 at $J_2^m(J')$ drops to a value similar to the one of L decoupled chains (see Fig. 5). For $M = 4$ and $L > M$, it is only for $J' \lesssim 0.9$ that the QDJS of $(\pi, 0)$ LRO becomes lower than the QDJS of $(0, \pi)$ LRO.

The boundary of the $(\pi, 0)$ Néel phase can be also estimated in the same way as for the (π, π) phase. For the $J_1 - J_2$ model it was found that J_2^{c2} occurs at a value slightly larger than $J_2^m \approx 0.6$, in the range $0.60 < J_2^{c2}(J' = 1) < 0.70$. Examination of the spectra for $J' < 1$ indicates that J_2^{c2} move closer to J_2^m as J' decreases with $J_2^{c2} \approx 0.5J'$ for $J' \rightarrow 0$. As at $J_2 = 0$, for Heisenberg chain coupled by J' interactions, it is likely that, at $J' = 0$, the 1D behavior of the single Heisenberg chain is unstable to J_2 interchain coupling leading to Néel LRO as soon as $J_2 > 0$.

Here too, the Néel LRO appears only in the limit of an infinite number of chain. The spin-gap remains finite at M fixed for $L \rightarrow \infty$. The ground-state is a non degenerate singlet. One has Haldane-like phases. Instead of the (π, π) Néel LRO one has the same phase as the phase of the M -leg (unfrustrated) ladder. In place of the $(\pi, 0)$ Néel LRO one has a phase, that is probably closely similar to the one of the spin- $M/2$ chain as found for the 2-leg and 3-leg ladders. These phases are analogues of the 'singlet' and 'Haldane' phases of 2-leg ladder. Like the 2-leg ladder they have likely an hidden topological LRO. This and their eventual relation to the chain of integer spins $S > 1$ for which string order parameters have been recently studied [36] deserves further investigation.

V. INTERMEDIATE REGION

Between these two regions of Néel behavior, there is an intermediate region for the range of parameters $J_2^{c1}(J') \leq J_2 \leq J_2^{c2}(J')$ where the spectra indicate an absence of Néel LRO when $L \rightarrow \infty$ and $M \rightarrow \infty$. Leaving the region of (π, π) Néel LRO by increasing J_2 at constant J' , the evolution of the energies of the lowest eigenstates in each S sector changes to $E(S) - E_0 \sim S$ for small values of S (see Fig. 10). This feature is an indication that the spin-gap opens for $L \rightarrow \infty$ and $M \rightarrow \infty$ [37] and one enters a magnetically disordered region. At the same time one observes a lowering of some singlet states. This linear behavior reaches its maximum extension for a value of J_2 that appears to coincide with J_2^m where it extends up to $S = M/2$ if $J' \lesssim 0.9$ as shown in Fig. 11 for $M = 4$ at $J' = 0.8$. Then, beyond J_2^m , the evolution of the lowest eigenenergies returns fast to $E(S) - E_0 \sim S(S+1)$ in the $(\pi, 0)$ Néel region which starts at J_2^{c2} , close to J_2^m .

The quantum numbers of the first excitations in each spin sector and the signs of the spin-spin correlations remain the same as in the (π, π) Néel region for $J_2 \lesssim J_2^m$

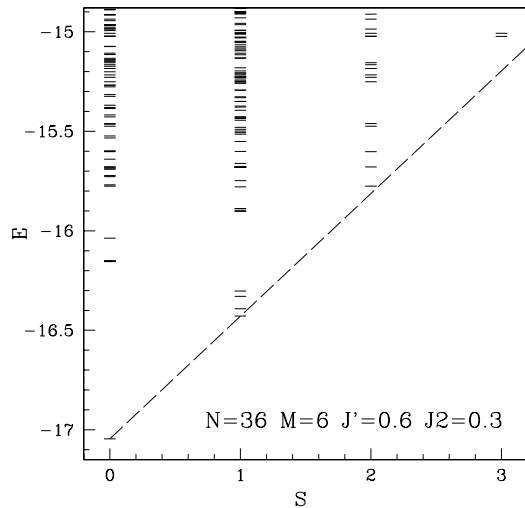


FIG. 10. Spectrum of eigenenergies vs total spin S for the $M = 6$ sample of $N = 36$ spins at $J' = 0.6$ and $J_2 = 0.3$. These values of J' and J_2 correspond to a point in the intermediate region (slightly) below the line $J_2^m(J')$ in Fig. 4 ($J_2^m(J' = 0.6) \approx 0.32$). The dashed line, fitted to the lowest $S = 1$ and $S = 0$ states, shows that the energy of the lowest states in each spin sector increase nearly as $\sim S$ at small S values.

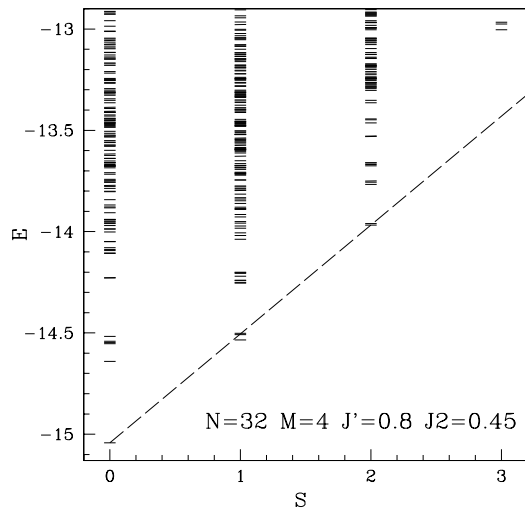


FIG. 11. Spectrum at $J' = 0.8$ and $J_2 = 0.45$ for the $N = 32$ sample of $M = 4$ chains

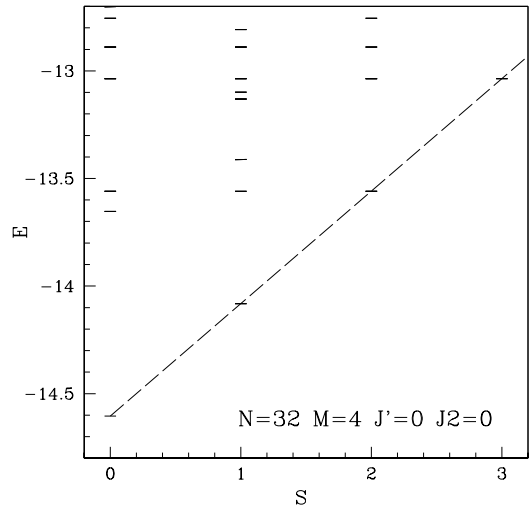


FIG. 12. Spectrum of decoupled chains for the $N = 32$ sample of $M = 4$ chains ($J' = 0$ and $J_2 = 0$). Note that the excited levels have a large degeneracy.

and are the same as in $(\pi, 0)$ region for $J_2 \gtrsim J_2^m$. The curve $J_2^m(J')$ is the analogue of the transition line of the classical model $J_2 = 0.5J'$. On this line the classical ground-state consist of decoupled chains. Then for $J_2 \approx J_2^m(J')$ one may notice features, in the spectra and the spin-spin correlations (observed for $M = 2, 4, 6$), that present certain similarities with those of M decoupled chains if $J' \lesssim 0.9$ (and those of L independent chains when $L > M$ and $J' \gtrsim 0.9$).

As indicated above, one has $E(S) - E_0 \sim S$ up to $S = M/2$, as for decoupled chains (see Fig. 12), which is what would result for independent magnetic excitations on the chains. Moreover, the very lowest eigenstates in each S sector belong to the same IR as those of a system of decoupled chains. For instance, the first triplets excitations is a set of M states with all wave-vectors of type (π, k_y) on the side the Brillouin zone which become quasi degenerate at $J_2 \approx J_2^m$ as shown in Fig. 13 for the $M = 4$, $N = 24$ sample at $J' = 0.8$. Similarly, first excitations at $S \geq 1$ and $S \leq M/2$ have same quantum numbers (wave vector, characters in point-group symmetries) as those of decoupled chains which result from the combination of first triplets excitations. The energies per spin (see Fig. 7) and the spin gaps at finite size are also quasi independent of the number of chains.

In addition the spin excitations appear quasi gapless. Although the finite-size spin-gaps are maximum for $J_2 \approx J_2^m$, as shown in Fig. 13, the analysis of the evolution of the spin-gap Δ^1 of the $M = 4$ samples with $1/L$ indicates that its value at $L \rightarrow \infty$ is minimum for $J_2 \approx J_2^m$ as for the 2-leg ladder [22,23]. If $J' \leq 0.6$ the scaling behavior of Δ^1 is quite similar to the one for the single chain (its evolution with $1/L$ is quasi linear with a very small *negative* curvature) and the extrapolated value

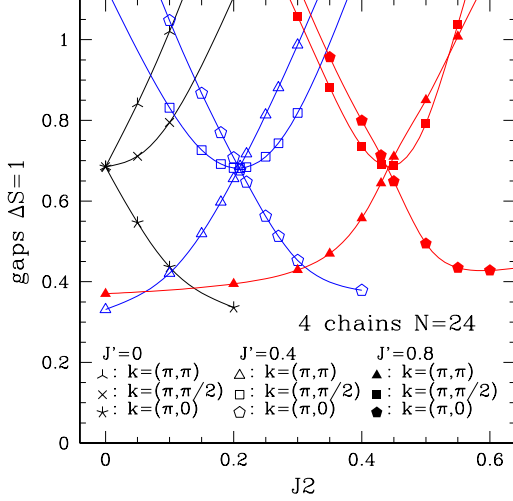


FIG. 13. Gaps to the 1th triplet ($\Delta S = 1$) vs J_2 for $N = 24$ samples with $M = 4$ (4 chains) and wave vectors $k = (\pi, k_y)$ on the side of the Brillouin zone if $J' = 0, 0.4, 0.8$. The lines are guides for the eye.

of Δ^1 is ≈ 0 . At $J' \gtrsim 0.8$ nevertheless the evolution of Δ^1 with $1/L$ turns to have a positive curvature and Δ^1 extrapolates to a finite (but small) value. This may be consistent with a spin-gap opening exponentially with increasing J' along $J_2^m(J')$ as predicted by NT at weak interchain coupling along $J_2 = 0.5J'$. However the spin-gap on $J_2^m(J')$ appears to remain very small up to large interchain coupling for $M \leq 4$ as found for $M = 2$ [23].

An apparent decoupling of the chains is also manifest in the spin-spin correlation between two spins at distance (l, m) :

$$s(l, m) = \langle \mathbf{S}_{0,0} \cdot \mathbf{S}_{l,m} \rangle. \quad (5.1)$$

Values of $s(l, m)$ for the $N = 32$ ($M=4$) sample are displayed vs J_2 at $J' = 0.8$ in Fig. 14 for pair of spins on the same ($m = 0$) or different ($m = 1, 2$) chains at short distances along the chains ($l \leq 2$). Since $s(l, m)$ decrease in magnitude at given m with increasing distance l along the chains these are the largest values of $s(l, m)$. $J_2^m \approx 0.45$ when $J' = 0.8$ and $N = 32$. As shown in Fig. 14 the inter-chain spin-spin correlations become very small at $J_2 = 0.45$: if $m \neq 0$, $s(l, m) \approx 0$ except between first neighbor spins which changes of sign at a slightly larger J_2 value.

Others features in the spectra nevertheless testify of interactions between the chains when $J_2 \approx J_2^m(J')$ for $M \leq 4$ as found for $M = 2$. Starting from situation of decoupled chains at $J' = 0$ and increasing J' along $J_2^m(J')$ one sees a modification of the structure of the eigenlevels above the most lowest eigenstates in each S sector. Levels which were degenerate for uncoupled chains move away from one-another. In particular, there is a number of singlet states which separate from the others and drift to-

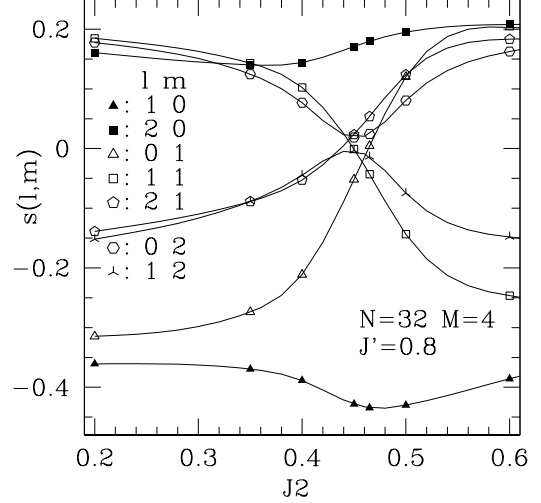


FIG. 14. Spin-spin correlations $s(l, m)$ (Eq 5.1) between spins at distance (l, m) vs J_2 for $N = 32$, $M = 4$, $J' = 0.80$. The lines are guides for the eye.

ward the ground state (from an energy \approx twice the spin-gap at $J' = 0$ to an energy \sim to the spin-gap at $J' = 0.8$ as shown in Fig. 11 for the $N = 32$ ($M = 4 \times L = 8$) sample). This could indicate a behavior at $J_2 \approx J_2^m$ that differs from the one of independent chains and raises the question whether it corresponds to the RVB state predicted by NT in the limit of small interchain coupling for $J_2 = 0.5J'$.

We investigate below successively the three cases $J_2 < J_2^m$, $J_2 \approx J_2^m$ and $J_2 > J_2^m$ in more detail. In order to be with an intermediate region sufficiently wide and to observe effects of interactions between the chains on small samples we shall mainly display results for a rather large $J' = 0.8$ value and discuss their evolution for smaller and larger values of J' .

A. $J_2 < J_2^m$

For $J_2 < J_2^m$ and not too close to J_2^m , the lowest excited singlet states, noted below $|1\rangle$, $|2\rangle$, $|3\rangle$ are: $|1\rangle$ in the trivial IR (quantum numbers: $\mathbf{k} = 0, R(\pi) = 1, \sigma = 1$), $|2\rangle$ [$\mathbf{k} = (\pi, 0), R(\pi) = -1, \sigma = 1$] and $|3\rangle$ [$\mathbf{k} = (0, \pi), R(\pi) = -1, \sigma = -1$].

Fig. 15 shows the evolution of the singlet-gaps Δ_i^0 from the ground-state $|0\rangle$ to the states $|i\rangle$ vs $1/L$ at $J' = 0.8$ and $J_2 = 0.4$ for the $M = 4, N = 16, 24, 32$ samples. The gaps appear to decrease monotonically. They evolve with an upward curvature vs $1/L$. As above we assume that the evolution of the gaps will remain similar at larger sizes as found for the 2-leg ladder. Lower bounds for the gaps are then obtained using linear extrapolations for $N > 32$. The lower bounds are positive values for Δ_1^0 and Δ_3^0 . This points to finite gaps Δ_1^0, Δ_3^0 . On the other

hand, the extrapolation suggests a possible vanishing of Δ_2^0 for $L \rightarrow \infty$. A similar analysis of these gaps for the $M = 6$, $N = 24, 36$ samples also point to the same conclusions for $L \rightarrow \infty$ if $M = 6$.

The vanishing of $\Delta_2^0(L \rightarrow \infty)$ for $M \leq 4$ may be questioned since the 2-leg ladder ($M = 2$) is known to be fully gapped [23]. The same analysis indeed shows that $\Delta_2^0(L \rightarrow \infty)$ is finite and rather large if $M = 2$ at $J' = 0.8$ and $J_2 = 0.4$. From this, it could be argued that $\Delta_2^0(L \rightarrow \infty)$ decreases with increasing values of M but remains finite for M finite. Our data, limited to small sizes cannot exclude this possibility. However, Δ_2^0 most likely vanish on J_2^m for $M \geq 4$ (see Sec. V B) and then, the range of values of J_2 where Δ_2^0 appear to vanish, starts at $J_2 \approx 0.35$ and extends beyond J_2^m till $J_2 \approx 0.5$ (see below) if $M = 4$. This interval is large which support a vanishing of Δ_2^0 on an extended range of values of J_2 . An other possibility, is that the value of J_2 at given J' beyond which $\Delta_2^0(L \rightarrow \infty)$ would vanish vary with M and drift toward J_2^m as M decreases. ED calculations indeed point out that $\Delta_2^0(L \rightarrow \infty)$ drops to a minimum at $J_2 \approx J_2^m$ for $M = 2$ where this gap is quasi-vanishing.

On the other hand, an analysis of the evolution of the spin-gap Δ^1 with $1/L$ show that it remain finite if $L \rightarrow \infty$ for $M = 4$ and $J_2 \leq J_2^m$. Besides the fact that $E(S)$ neither evolve as $E(S) - E_0 \sim S(S+1)$ or as $E(S) - E_0 \sim S$ indicate that the spin-gap is finite for $L \rightarrow \infty$ and $M \rightarrow \infty$.

All together, the ED results suggest the occurrence of a $(\pi, 0)$ VBC LRO at $J' = 0.8$ for $J_2 \gtrsim 0.35$, breaking translational symmetry in the horizontal direction with a twice degenerate ground-state, gapped to others singlet and magnetic excitations, possibly as soon as $M = 4$ when M is even, and most likely when $M \rightarrow \infty$.

The patterns of dimer-dimer correlations

$$D(i, j; k, l) = \langle (\mathbf{S}_i \cdot \mathbf{S}_j)(\mathbf{S}_k \cdot \mathbf{S}_l) \rangle - \langle \mathbf{S}_i \cdot \mathbf{S}_j \rangle \langle \mathbf{S}_k \cdot \mathbf{S}_l \rangle \quad (5.2)$$

between valence bonds on pairs sites (i, j) and (k, l) are displayed in Fig. 16 for the $N = 32$ sample at $J' = 0.8$ and $J_2 = 0.4$. Fig. 16(a) is consistent with a columnar $(\pi, 0)$ VBC LRO although the correlations between horizontal dimers on different chains are rather small. Fig. 16(b) shows nonetheless correlations between vertical dimers that are not smaller than those between horizontal dimers and that could be consistent with a columnar $(0, \pi)$ VBC LRO. This may be related to the fact that Δ_2^0 at $L = 8$ is still higher than the singlet gaps Δ_1^0, Δ_3^0 . It is the extrapolation of Δ_1^0, Δ_3^0 at $L \rightarrow \infty$ to finite values that exclude a $(0, \pi)$ VBC LRO for $J' = 0.8$. In Fig. 16 we see that the dimer correlations are strongest between pair of bonds on adjacent chains and much weaker otherwise. These features reinforce with increasing J_2 and will be maximum at $J_2 \approx J_2^m$. Simultaneously, the extrapolated values of Δ_1^0, Δ_3^0 at $L \rightarrow \infty$ decrease toward zero. If $J' \lesssim 0.9$, the same features for the singlet gaps and the dimer correlations remain in the intermediate region for $J_2 < J_2^m$.

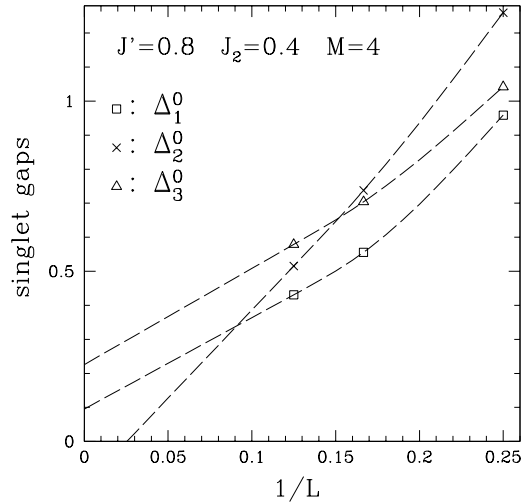


FIG. 15. Singlet-gaps Δ_i^0 at $J' = 0.8$ and $J_2 = 0.4$ vs $1/L$ for for $N = 16, 24, 32$ samples of $M = 4$ chains. The dashed lines are spline fits to the data for $N \leq 32$ followed by linear extrapolation for $N > 32$.

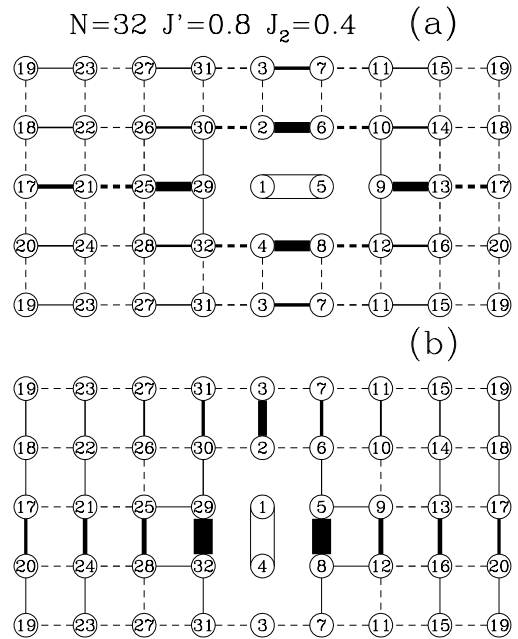


FIG. 16. Dimer-dimer correlation function $D(i, j; k, l)$ (Eq 5.2) of a dimer on a reference pair of sites (i, j) with a dimer on a pair of sites (k, l) for $N = 32$, $J' = 0.80$, $J_2 = 0.4$. The reference bond: $(1, 5)$ in (a), $(1, 4)$ in (b), is represented by a double line. A solid (dashed) line means a positive (negative) value of D . The thickness of the line is proportional to the magnitude of D .

Interchanging the role of J and J' in the preceding analysis points out that a $(0, \pi)$ VBC could occur for finite L if $M \rightarrow \infty$ at sufficiently large J' . On the other hand, VBC LRO for finite M , in the limit $L \rightarrow \infty$, may be excluded at large J' . As mentioned in Sec. II, there is a crossover in the range $0.9 < J' < 1$ to a situation where the systems, for an aspect ratio $M/L < 1$, may be best viewed as an array of L chains in the vertical directions. For larger J' the evolutions of the above singlet gaps with $1/L$ show that Δ_2^0 opens and all gaps are finite at $L \rightarrow \infty$ for $M = 4, 6$. The $(\pi, 0)$ VBC LRO then disappear. In particular, there is no VBC LRO for M finite if $J' = J = 1$. The gaps nevertheless decrease at fixed L for increasing M and the value of J' where the crossover occurs for $M/L < 1$ shifts with increasing values of M to $J' = J$ for $M/L \rightarrow 1$. Thus $(\pi, 0)$ VBC LRO may extend to $J' \rightarrow J$ if $L, M \rightarrow \infty$ where it would be degenerate with $(0, \pi)$ VBC LRO.

However an analysis of the evolution of the gaps Δ_1^0 , Δ_2^0 , Δ_3^0 with the size of the samples one may study by the ED method do not allow to conclude that these gaps vanish at $J' = J = 1$ for $N \rightarrow \infty$, as required for the four-fold degenerate columnar order corresponding to degenerate $(\pi, 0)$ and $(0, \pi)$ orders.

It could be possible that one has $(\pi, 0)$ LRO for $J' < 1$ and $(0, \pi)$ LRO for $J' > 1$ but that VBC LRO vanishes on the line $J' = J$. However, the transition out of $(\pi, 0)$ VBC phase might be first order: the gap Δ_2^0 appears to jump to a large value going through the transition by increasing J' . The order parameter would then be finite on the transition line and, if this transition line extends to the line $J' = J$ for $L = M \rightarrow \infty$, it would imply that the four-fold columnar order occurs on the line $J' = J$ where the $J - J' - J_2$ model reduces to the $J_1 - J_2$ model. A picture of the dimer correlations similar to the one observed above for at $J' = 0.8$ and $J_2 = 0.4$ with strongly correlated pair of chains has been found in dimer series expansions approaches for the $J_1 - J_2$ model when $0.4 \lesssim J_2 \lesssim 0.5$ [10]. The pattern of dimer correlations in one of the four-fold degenerate columnar states would then be reminiscent of the one off the line $J' = J$.

The locations of the end of the (π, π) Néel phase (for $M \rightarrow \infty$) and of the beginning of the $(\pi, 0)$ VBC phase may differ [16]. They are difficult to estimate accurately from ED calculations with the present sizes but are probably very close or coincident as conjectured for the $J_1 - J_2$ model [16].

B. $J_2 \approx J_2^m$

J_2^m is ≈ 0.45 at $J' = 0.8$. At $J' = 0.8$ and $J_2 = 0.45$, the evolution of the gaps to the first triplet for $M = 4$ with $1/L$ (not shown) indicates that the spin-gap remains finite $L \rightarrow \infty$ although it has become much smaller than at $J_2 < J_2^m$. The new feature is the appearance of other

singlet states in the low part of the spectrum which, at first sight, appear to form a set of states separated from the singlet continuum (see Fig. 11). This set includes the lowest states with wave vector $\mathbf{k} = (0, k_y)$ [$k_y = 2\pi m/M$ $m \in [M/2 - 1, \dots, M/2]$] even under σ : the two states noted $|4 \rangle$ [$\mathbf{k} = (0, \pm\pi/2)$, $\sigma = 1$] if $M = 4$ or the states [$\mathbf{k} = (0, \pm\pi/3)$, $\sigma = 1$], [$\mathbf{k} = (0, \pm 2\pi/3)$, $\sigma = 1$] if $M = 6$, then noted $|4 \rangle$ and $|4' \rangle$. If $M = 4$, there also the 2th excited state in the trivial IR, noted $|5 \rangle$, just above the states $|1 \rangle$, $|2 \rangle$, $|3 \rangle$, $|4 \rangle$ whereas if $M = 6$, there are also the lowest states [$\mathbf{k} = (\pi, \pm\pi/3)$, $\sigma = -1$], then noted $|6 \rangle$. Next if $M = 4$, one has just below the singlet continuum a state, noted $|6 \rangle$, with [$\mathbf{k} = (\pi, \pm\pi/2)$, $\sigma = -1$], whereas if $M = 6$, one finds, adjacent to the singlet continuum the 2th excited state in the trivial IR (noted $|5 \rangle$) followed by states with wave vectors $\mathbf{k} = (0, k_y)$.

This low energy spectrum is different from the one for independent chains to which it may be compared. In the case of decoupled chains the lowest singlets above the ground-state (see Fig. 12) is the degenerate set \mathcal{S}_1 of M states with wave vectors $\mathbf{k} = (\pi, k_y)$ ($k_y = 2\pi m/M$ $m \in [M/2 - 1, \dots, M/2]$) which consists of $|2 \rangle$, $|6 \rangle$ and the state [$\mathbf{k} = (\pi, \pi)$, $R(\pi) = -1, \sigma = 1$], noted $|8 \rangle$ if $M = 4$ whereas it includes $|2 \rangle$, $|6 \rangle$, $|8 \rangle$ and the state [$\mathbf{k} = (\pi, \pm 2\pi/3)$, $\sigma = -1$] noted $|8' \rangle$ if $M = 6$. These states correspond to $S = 0$ lowest excitations along individual chains (which wave vector differs from the one of the ground-state by $\Delta k = \pi$). Just above this set, one has the set \mathcal{S}_2 of C_M^2 degenerate states with wave vector $\mathbf{k} = (0, k_y)$ which consists of $|1 \rangle$, $|3 \rangle$, $|4 \rangle$, $|5 \rangle$ and the state [$\mathbf{k} = (0, \pi)$, $R(\pi) = 1, \sigma = 1$], noted $|7 \rangle$ if $M = 4$ (6 states), whereas if $M = 6$, it includes $|1 \rangle$, $|3 \rangle$, $|4 \rangle$, $|4' \rangle$, $|5 \rangle$, $|8 \rangle$, a 3th state in the trivial IR, a second state in the same IR as $|4 \rangle$ and two states in the same IR as $|4' \rangle$ (15 states). These states correspond to the combination of two $S = 1$ lowest excitations on different chains in a total singlet state (the lowest $S = 1$ excitations of the single chain has a wave vector which differs from the one of the ground-state by $\Delta k = \pi$). Third, one has a set \mathcal{S}_3 of M states with wave vectors $\mathbf{k} = (\pi, k_y)$. These states are: [$\mathbf{k} = (\pi, 0)$, $R(\pi) = -1, \sigma = -1$], [$\mathbf{k} = (\pi, \pi/2)$, $\sigma = 1$], [$\mathbf{k} = (\pi, \pi)$, $R(\pi) = -1, \sigma = -1$] if $M = 4$. They correspond to the combination of three lowest $S = 1$ excitations on different chains. Above \mathcal{S}_3 appear sets of states with wave vectors inside the Brillouin zone which involve higher excitations on individual chains at $\Delta k \neq \pi$ and appear to form a continuum. At small values of L , the sets of states \mathcal{S}_1 , \mathcal{S}_2 remain well separated from this continuum which starts at \mathcal{S}_3 . Yet, in the limit $L \rightarrow \infty$ the gaps to the states of \mathcal{S}_1 , \mathcal{S}_2 , \mathcal{S}_3 , vanishes as the gaps to the lowest $S = 0, 1$ excited states of a single chain. The excited states form a gapless continuum adjacent to the ground-state.

On the line of maximum frustration, the degeneracy in the sets \mathcal{S}_1 and \mathcal{S}_2 appears to be lifted by interchain couplings. Fig. 17 shows the variation of the gaps Δ_i^0 for the $N = 32$ sample vs J' for values of $J_2 \approx J_2^m(J')$. The

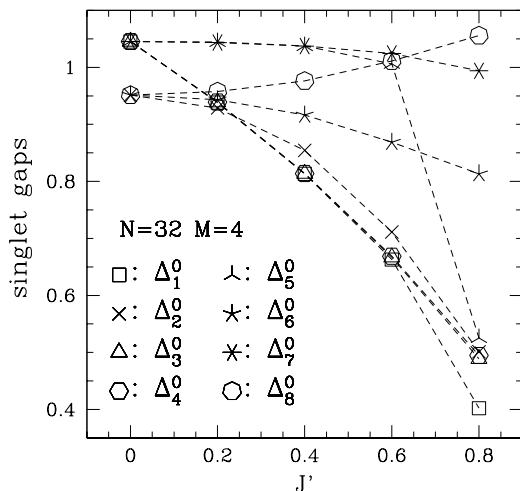


FIG. 17. Singlet-gaps Δ_i^0 (see text) of the $N = 32$ $M = 4$ sample vs J' for values of $J_2 \approx J_2^m(J')$. The dashed lines are guide to the eyes.

three states $|2\rangle$, $|6\rangle$, $|8\rangle$ of \mathcal{S}_1 splits. The gaps Δ_2^0 , Δ_6^0 decrease with increasing J' , while Δ_8^0 increases. The set \mathcal{S}_2 separate in two groups. The first group consists of the states $|1\rangle$, $|3\rangle$, $|4\rangle$ which remain very close in energy up to $J' = 0.6$. Their gaps decrease with increasing J' . The second group includes the states $|5\rangle$ and $|7\rangle$ which remain at approximately the same energy up to $J' \sim 0.6$. Beyond this value, $|5\rangle$ decreases rather abruptly to an energy close to the first group, a drop which may be attributed to the proximity of the range of values of $0.9 < J' < 1$ where the crossover to the large J' behavior occurs (for $J' = 0.9$ additional singlet states which evolve from the lowest singlet states of L independent chains will begin to appear in the low part the spectrum if $N = 32$). A similar splitting also occurs in most of the sets of states which are above \mathcal{S}_3 (the states of \mathcal{S}_3 remain nevertheless quasi-degenerate). The energy of some of these states and the energy of the states of \mathcal{S}_3 decrease with increasing J' and become comparable to the energy of the the states $|5\rangle$, $|7\rangle$, $|8\rangle$ for $J' \sim 0.6$. Yet, up to $J' = 0.4$ the evolution vs $1/L$ of the gaps Δ_i^0 to the states of \mathcal{S}_1 and \mathcal{S}_2 shows that these splitting are much reduced for $L \rightarrow \infty$. All the gaps to the states of \mathcal{S}_1 , \mathcal{S}_2 and \mathcal{S}_3 extrapolate to ≈ 0 . The singlet spectrum thus remains close to the one of independent chains. The finite-size results give nevertheless a first indication that the splitting of the states in \mathcal{S}_1 , \mathcal{S}_2 will subsist for $L \rightarrow \infty$. A differentiation in the extrapolated values of the gaps becomes more visible at larger J' values.

Fig. 18 shows the evolution of the singlet-gaps Δ_i^0 vs $1/L$ for the $M = 4$ samples at $J' = 0.8$ and $J_2 = 0.45$. The evolutions of the Δ_i^0 still remain quasi-linear with $1/L$ if $L \leq 8$ ($N \leq 32$) on $J_2^m(J')$ up to $J' = 0.8$. A curvature is hardly visible. But, since a linear extrapolation

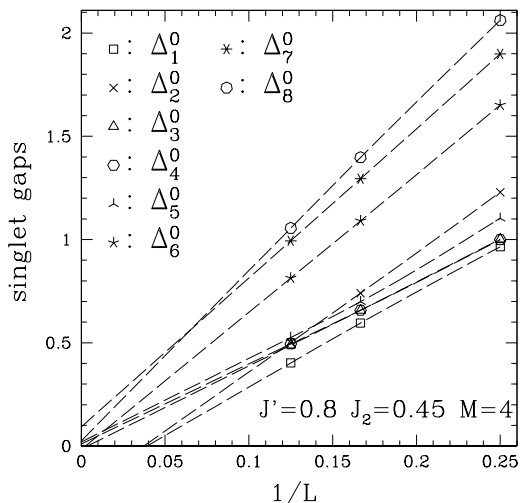


FIG. 18. Singlet-gaps Δ_i^0 (see text) at $J' = 0.8$ and $J_2 = 0.45$ vs $1/L$ for for $N = 16, 24, 32$ samples of $M = 4$ chains. The dashed lines are spline fit to the data for $N \leq 32$ followed by linear extrapolation for $N > 32$.

for $N > 32$ would leads to negative values for Δ_1^0 , Δ_2^0 , Δ_3^0 , Δ_6^0 , an upward curvature may be inferred for these gaps. This affects the precision of the extrapolations for $L \rightarrow \infty$ but one may conjecture, in view of Fig. 18, that not only Δ_2^0 still likely vanishes as at $J_2 = 0.4$, but also Δ_1^0 , whereas the other Δ_i^0 are very small and some may vanishes. This could be the case of Δ_3^0 , Δ_6^0 which extrapolate to negative values and probably Δ_4^0 which follow closely Δ_3^0 for all sizes if $J' \leq 0.8$. The vanishing of Δ_6^0 is nonetheless uncertain as the degeneracy of state $|6\rangle$ with the state $|2\rangle$ seems to be lifted on the line $J_2^m(J')$. But Δ_7^0 , Δ_8^0 and probably Δ_5^0 which extrapolate above Δ_4^0 remain finite. Thus the degeneracies which occur for decoupled chains are lifted. Nonetheless these gaps remain probably very small which suggest that they open exponentially like the spin-gap. The gaps to the states at the bottom of the singlet continuum are also small. Those to the states of \mathcal{S}_3 extrapolate to quasi-vanishing values. The spectrum appears to be gapless or quasi-gapless.

The exact degree of ground-state degeneracy is difficult to ascertain, especially for $M = 6$. The most likely vanishing gaps are Δ_1^0 , Δ_2^0 , Δ_3^0 , Δ_4^0 , Δ_6^0 . for $M = 4$. This would lead to a $2^{M-1} = 8$ ground-state degeneracy. Yet the degeneracy would be limited to 6 if Δ_6^0 remains finite. Besides the gaps to the lowest states in the singlet continuum appear to be quasi-vanishing. For $M = 6$, the extrapolations of the singlet gaps, although even more unaccurate than for $M = 4$, also indicate a large ground-state degeneracy and a gapless continuum of singlet excitations adjacent to the ground-state. This also suggests a spectrum that correspond closer to the one of the RVB state of NT than to the one of independent chains.

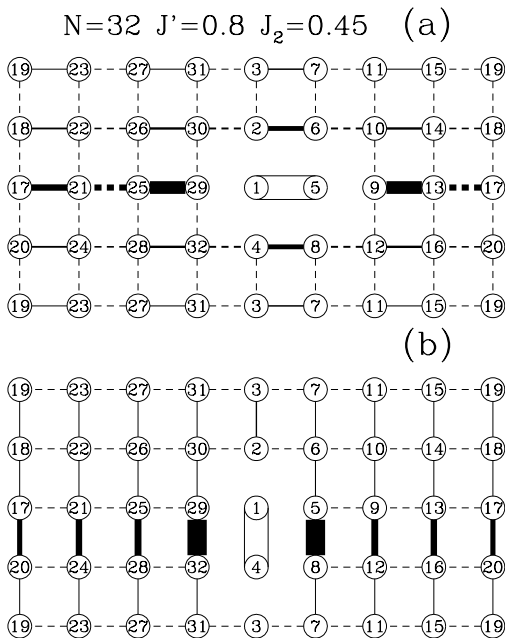


FIG. 19. Dimer-dimer correlation function (see Fig 16) for $N = 32$, $J' = 0.80$ $J_2 = 0.45$.

This degeneracy of additional singlet states is accompanied with a modification of the pattern of the dimer-dimer correlations $D(i, j; k, l)$ as shown for $N = 32$ in Fig. 19. Dimer-dimer correlations $D(1, 5; k, l)$ between a reference horizontal pair (1, 5) and a pair (k, l) on the same chain remain strong but have now become extremely small otherwise, much weaker than for $J_2 = 0.4$, as shown in Fig. 19(a). As shown in Fig. 19(b), this is also the case for dimer-dimer correlations $D(1, 4; k, l)$ between a vertical dimer on a pair of chains and vertical dimer on a different pair of chains, whereas $D(1, 4; k, l)$ remain of significant magnitude for pairs of dimers joining the same chains. Fig. 19(a)(b) give a picture of strongly correlated pairs of adjacent chains, decorrelated from one pair to the next with dimer long range correlations along individual chains and along the rungs of pairs of adjacent chains. This pairing is reminiscent of the RVB state of NT.

The ED results thus indicate a behavior close to the one of independent chains on $J_2^m(J')$ up to very large interchain coupling but which differs. Instead, they suggest that the RVB behavior predicted by NT at weak interchain coupling may be realized and also extends at large interchain coupling, perhaps up to $J' = 0.8$, if $J_2 \approx J_2^m(J')$.

The extension of the RVB state on $J_2^m(J')$ would however have an upper limit. For $J' \gtrsim 0.9$ the evolution of the singlet gaps vs $1/L$ show that they are clearly finite if $L \rightarrow \infty$ for $M = 4$. This would imply a transition on $J_2^m(J')$. The transition might be discontinuous as the gaps seems to open abruptly. An alternative possibility could be that the RVB state is only approximatively realized on $J_2^m(J')$. The degeneracy of the RVB state would be progressively lifted with increasing J' but slower than the degeneracy corresponding to the independent chain

behavior.

The ED results on the $M = L$ samples of $N = 16, 36$ spins at $J' = J$ indicate that the behavior of the $J_1 - J_2$ model for J_2^m differs from the one at $J' < J$. But several features reminiscent of this state subsists. The lowest triplet excitations have only a small dispersion on the boundary of the Brillouin zone. The singlet spectrum at finite size is rather similar to the one for $J' < J$: one finds low lying states with wave vector on the side of the Brillouin zone in addition to $|1 \rangle$, $|2 \rangle$, $|3 \rangle$ (degenerate with $|2 \rangle$) which would allow to form a four-fold degenerate columnar VBC. The $J_1 - J_2$ model for J_2^m , if it displays VBC order, is nonetheless close to a state with a spin-liquid behavior at this point of the phase diagram.

C. $J_2 > J_2^m$

The behavior predicted by NT is also most likely limited to the line $J_2^m(J')$. Increasing J_2 at fixed J' one finds a narrow region with a different behavior before reaching the region where the spectra display the features of the $(\pi, 0)$ Néel phase. The spin-spin correlations $s(l, m)$ (Eq. 5.1) at $J' \leq 0.8$ have now the same signs as in the $(\pi, 0)$ Néel phase: $s(l, m) \sim -1^l$, alternating in sign in the horizontal direction and being ferromagnetic along vertical lines. Fig. 20 shows the evolution of the singlet gaps at $J' = 0.8, J_2 = 0.47$ for $M = 4$ which indicate that singlet gaps have opened except Δ_1^0 and Δ_2^0 which may still vanish. This excludes an eight-fold degeneracy of the ground-state. But the exact degeneracy of the ground-state is difficult to ascertain. The region is very narrow (all singlet gaps are clearly finite at $J_2 = 0.5$ when $J' = 0.8$), much narrow than the region between the (π, π) Néel phase and the line $J_2 = J_2^m(J')$. Due to the proximity of the line $J_2 = J_2^m(J')$ where Δ_1^0 , Δ_2^0 would vanish it is difficult to conclude whether both Δ_1^0 and Δ_2^0 really vanishes.

The patterns of dimer-dimer correlations are shown in Fig. 21 for $N = 32$ and $M = 4$ at $J' = 0.8, J_2 = 0.47$. The correlations between horizontal dimers in Fig. 21(a) display a similar alternation of sign as in Fig. 16(a) and could be compatible with a columnar $(\pi, 0)$ VBC LRO, although they have a small magnitude if the bonds are on different chains.

As the shortest pair of spins with the next largest AF spin-spin correlations are on the diagonals of a square, whereas the vertical nearest neighbor spins are ferromagnetically correlated, we have displayed the correlations between diagonal bonds (Fig. 21(b)) and between diagonal and horizontal bonds (Fig. 21(c)).

As shown in Fig. 21(b), the correlations between diagonal bonds $D(1, 6; k, l)$ do not show a clear modulation in their magnitudes neither in the horizontal, the vertical or the diagonals directions. $D(1, 6; k, l)$ is small except for bonds linking two adjacent chains. There subsists a

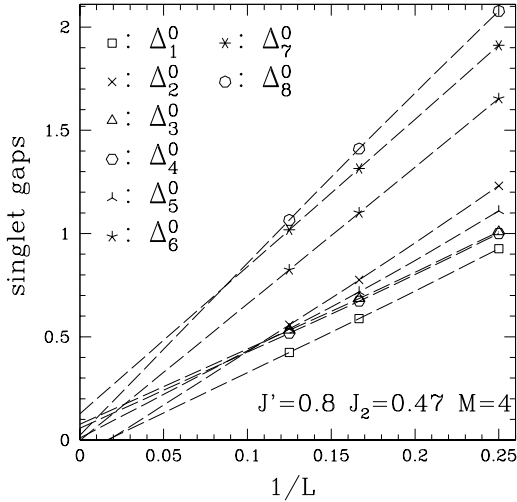


FIG. 20. Same as Fig. 18 at $J' = 0.8$ and $J_2 = 0.47$.

tendency of pairs of adjacent chains to associate as seen in Fig. 19(b). The correlations are then rather similar to those in the 'Haldane phase' of the two-leg ladder. There is no visible tendency of the diagonal bonds to order.

As shown in Fig. 21(c), the correlations between a horizontal bond and a diagonal bond in the same column are negative and there is a sign alternation of the correlations between an horizontal bond and diagonal bonds in the horizontal direction similar to alternation in Fig. 21(a), compatible with a breaking of translational symmetry in the horizontal direction.

A vanishing of Δ_1^0 , Δ_2^0 would lead to a three-fold ground-state degeneracy, but the pattern of dimer-dimer correlations do not indicate a VBC LRO with a three-fold degeneracy of states $|0\rangle$, $|1\rangle$, $|2\rangle$.

On the other hand, a columnar VBC LRO with plaquette modulation, which would lead to an additional translational symmetry breaking in the vertical direction, appears also unlikely for $J' \leq 0.8$ in view of the pattern of dimer-dimer correlations and the fact that the gap Δ_3^0 to the singlet state $|3\rangle$ with wave-vector $(0, \pi)$ is finite.

If there is VBC LRO, it is most probably a $(\pi, 0)$ like VBC LRO. It will be associated with a vanishing of Δ_2^0 whereas Δ_1^0 will be finite. The small but noticeable upward curvature in the evolution of Δ_1^0 in Fig. 20 supports indeed that Δ_1^0 might be finite for $L \rightarrow \infty$ in this region for $J' = 0.8$. As for $J_2 < J_2^m$, the $(\pi, 0)$ VBC LRO disappears for $J' < 1$ if M is finite but could extend for $J' \rightarrow 1$ if $M = L \rightarrow \infty$.

The occurrence of a $(\pi, 0)$ VBC at $J_2 < J_2^m(J')$ would mean that there is the same kind of VBC LRO on both sides of $J_2^m(J')$ for $M \geq 4$. The state for $J_2 > J_2^m(J')$ could however differs from the state for $J_2 < J_2^m(J')$ by some non-local order parameter similar to those of the 'singlet state' and the 'Haldane state' of the two-leg ladder as conjectured at the end of Sec. IV for the phases

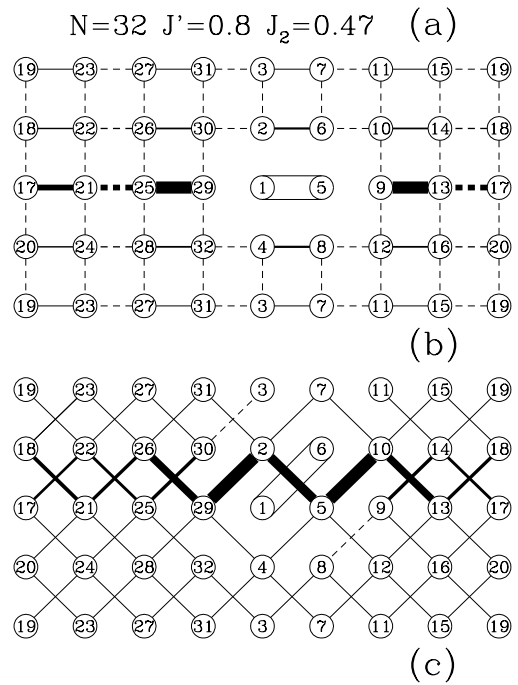


FIG. 21. Dimer-dimer correlation functions (see Fig 16) for $N = 32$, $J' = 0.80$ $J_2 = 0.47$.

at finite $M > 2$ on both sides of the intermediate region.

VI. SUMMARY

Exact diagonalization calculations provide support that the RVB behavior predicted by Nersesyan and Tsvelik in the $J - J' - J_2$ model at $J_2 = 0.5J' \ll J$ may be realized and extends along a curve coincident with the line of maximum frustration $J_2^m(J')$ where it subsists up to large interchain coupling for an even number M of chains of length $L \rightarrow \infty$. The line $J_2^m(J')$ is the analogue of the transition line $J_2 = 0.5J'$ in the classical model on which the chains decouple. The independent chain behavior appears destabilized by quantum fluctuations.

The line $J_2^m(J')$ is located in an intermediate region of the phase diagram where the present results suggest that the ground-state displays a columnar $(\pi, 0)$ valence bond long range order. This region of columnar order will have a finite width as soon as $M \geq 4$ and extends on both sides of $J_2^m(J')$ up to a value of J' close but smaller than J for finite M , that increase with M and approach $J' = J$ for $M = L \rightarrow \infty$. It separates two phases that are fully gapped Haldane like phases for finite M and evolves respectively to the (π, π) and $(\pi, 0)$ Néel phases

for $M \rightarrow \infty$. The Haldane like phases have probably a topological order. Its nature for $M > 2$ deserves further investigation.

The occurrence of a columnar order for J' smaller than J , next to the Néel phase, agrees with the scenario deduced from large- N approaches that valence bond crystal order is expected after the destabilization of a collinear AF Néel phase. It is possible that the columnar order may extend for $J' \rightarrow J$ if $M = L \rightarrow \infty$ and that this scenario may be realized also in the $J_1 - J_2$ model which corresponds to $J' = J$. The behavior of the $J - J' - J_2$ model in the intermediate region for $J' \rightarrow J$ requires nonetheless further study to confirm this hypothesis.

The exact diagonalization method is limited to systems of small sizes. The extrapolations to the infinite length limit are affected by uncertainties. Indeed, some one dimensional systems requires data at very large lengths to allow a reliable extrapolation to the infinite length limit. For certain systems there may be a crossover in the scaling behavior of the gaps at a very large length as shown for instance in Ref. [38] where some gaps do not decrease monotonically with the length beyond a certain length. For the present model we have assumed a monotonically decreasing smooth evolution of the gaps with increasing length. The assumption appears reasonable in view of the data available at large lengths in the case of two chains (the 2-leg ladder). Yet, a small change in the evolution of the gaps at very large lengths is not to be excluded for those gaps that appear to extrapolate to vanishing or quasi vanishing values. The scaling behavior of the gaps to the low lying excited states as a function of the number of chains deserves further studies. In particular, calculations using an approach that can deal with very large systems, like possibly the DMRG method, would be worth to firmly establish whether the gaps that have been conjectured to extrapolate to zero really vanish or are just small but finite in the thermodynamic limit and thus check the exact degeneracy of the ground state on the line of maximum frustration.

This study was limited to the case of AF couplings. Yet, the $J - J' - J_2$ model with AF intrachain coupling ($J > 0$), but interchain couplings (J', J_2) that are either or both ferromagnetic (FM) is also of interest [39]. Indeed, FM couplings may be relevant to modelize certain 2-leg ladder materials [40] and might be introduced to describe some M -leg compounds.

Classically, the ground-state of the $J - J' - J_2$ model remains AF for $J' > -1$ and $J_2 > -0.5$ (if $J = 1$). It is the (π, π) Néel state for $J_2 < 0.5J'$, the $(\pi, 0)$ Néel state for $J_2 > 0.5J'$, and the J chains stay decoupled for $J_2 = 0.5J'$.

The spin-1/2, 2-leg ladder (with FM J' and/or J_2) has been studied by bosonization [41] and DMRG [42] calculations. These studies showed that the singlet and Haldane phases extends for $J', J_2 < 0$, separated by a transition line which is the continuation of the boundary line for $J', J_2 > 0$. This transition line is also the line of the points of maximum frustration $J_2^m(J')$. The

transition line, however, does not deviate from the classical boundary line $J_2 = 0.5J'$ and the transition appears to be 2nd order for $J', J_2 \leq 0$, instead of 1th order for $J', J_2 > 0$. In the bosonization approach, the interchain interaction, derived at 1th order, proportional to $g = J' + 2J_2$ which now turn to be < 0 , is then irrelevant and does not open a gap. The system is predicted to be critical and to consist of independent chains [43].

A similar change of sign of the interchain interactions appears in the bosonization approach of NT if $J_2 = 0.5J' < 0$ for the 4-leg ladder. The same critical behavior could occur on the transition line in the 4-leg ladder and perhaps for M -leg ladders ($M > 2$ even). Preliminary calculations indicate that the curve $J_2^m(J')$ also remains on the classical boundary line for $M = 4$, where the model might be critical, perhaps down to $J' = -0.8$. The model may exhibit "sliding Luttinger spin-liquid" behavior as proposed for the crossed chain model [44], at least for not too strong interchain interactions. On the line $J_2 = 0.5J'$, the lowest energies $E(S)$ in spin sector S evolves linearly with S . For $M \rightarrow \infty$, there may be also an intermediate region with a spin-liquid state around this line in between the Néel phases, where $E(S) - E_0 \sim S(S+1)$. This issues deserve further study.

Acknowledgments: I thank Patrick Azaria, Philippe Lecheminant and Claire Lhuillier for fruitful discussions. I thank the Aspen Center for Physics, where this work was continued, for hospitality. Computations were performed at The Centre de Calcul pour la Recherche de l'Université Pierre et Marie Curie and at the Institut de développement des Recherches en Informatique Scientifique du CNRS under contract 981052.

-
- [1] N. Read and S. Sachdev, Phys. Rev. B **42**, 4568 (1990).
 - [2] N. Read and S. Sachdev, Phys. Rev. Lett. **66**, 1773 (1991).
 - [3] S. Sachdev and K. Park, Annals of Physics (N.Y.) **298**, 58 (2002).
 - [4] J.-B. Fouet, P. Sindzingre, and C. Lhuillier, Eur. Phys. J. B **20**, 241 (2001).
 - [5] P. Sindzingre, J.-B. Fouet, and C. Lhuillier, Phys. Rev. B **66**, 174424 (2002).
 - [6] J.-B. Fouet, M. Mambrini, P. Sindzingre, and C. Lhuillier, Phys. Rev. B **67**, 054411 (2003).
 - [7] A. Läuchli, S. Wessel and M. Sigrist, Phys. Rev. B **66**, 014401 (2002).
 - [8] H. Schulz and T. A. L. Ziman, Eur. Phys. Lett. **18**, 355 (1992)
 - [9] H. Schulz, T. A. L. Ziman and D. Poilblanc, J. Phys. I (France) **6**, 675 (1996).
 - [10] R. R. P. Singh, Z. Weihong, C. J. Hamer, and J. Oitmaa, Phys. Rev. B **60**, 7278 (1999).
 - [11] V. N. Kotov, Jaan Oitmaa, Oleg Sushkov, Zheng Weihong, Phil. Mag. B **80**, 1483 (2000).

- [12] L. Capriotti and S. Sorella, Phys. Rev. Lett. **84**, 3173 (2000).
- [13] M. S. L. du Croo de Jongh, J. M. J. van Leeuwen, W. van Saarloos, Phys. Rev. B **62**, 14844 (2000).
- [14] O. P. Sushkov, J. Oitmaa, and Z. Weihong, Phys. Rev. B **63**, 104420 (2001).
- [15] L. Capriotti, F. Becca, A. Parola and S. Sorella, Phys. Rev. Lett. **87**, 097201 (2001).
- [16] O. P. Sushkov, J. Oitmaa, and Zheng Weihong, Phys. Rev. B **66**, 054401 (2002).
- [17] L. Capriotti, F. Becca, A. Parola and S. Sorella, Phys. Rev. B **67**, 212402 (2003).
- [18] A. A. Nersesyan and A. M. Tsvelik, Phys. Rev. B **67**, 024422 (2003).
- [19] F. A. Smirnov and A. M. Tsvelik, Phys. Rev. B **68**, 144412 (2003).
- [20] M. J. Bhaseen and A. M. Tsvelik, Phys. Rev. B **68**, 094405 (2003).
- [21] Zheng Weihong, V. Kotov and J. Oitmaa Phys. Rev. B **57**, 11439 (1998).
- [22] Xiaoqun Wang, condmat/9803290 (unpublished); Mod. Phys. Lett. B **14**, 32 (2000).
- [23] T. Hakobyan, J. H. Hetherington, and M. Roger, Phys. Rev. B **63**, 144433 (2001)
- [24] Dave Allen, F. H. L. Essler and A. A. Nersesyan, Phys. Rev. B **61**, 8871 (2000).
- [25] Xiaoqun Wang, N. Zhu and C. Chen, Phys. Rev. B **66**, 172405 (2002).
- [26] F. D. M. Haldane, Phys. Lett. **93A**, 464 (1983)
- [27] S. R. White, R. M. Noack, and D. J. Scalapino, Phys. Rev. Lett. **73**, 886-889 (1994).
- [28] M. Greven, R. J. Birgeneau, U.-J. Wiese, Phys. Rev. Lett. **77**, 1865 (1996).
- [29] B. Frischmuth, B. Ammon, and M. Troyer, Phys. Rev. B **54**, R3714 (1996).
- [30] A. W. Sandvik, Phys. Rev. Lett. **83**, 3069 (1999).
- [31] S. R. White, Phys. Rev. B **53**, 52 (1996).
- [32] P. Azaria, P. Lecheminant and A. A. Nersesyan, Phys. Rev. B **58**, R8881 (1998)
- [33] S. Moukouri, cond-mat/0305608 (unpublished).
- [34] B. Bernu, C. Lhuillier, and L. Pierre, Phys. Rev. Lett. **69**, 2590 (1992).
- [35] P. Hasenfratz and F. Niedermayer, Z. Phys. B. Condensed Matter **92**, 91 (1993).
- [36] Shaojin Qin, Jizhong Lou, Liqun Sun and Changfeng Chen, Phys. Rev. Lett. **90**, 067202 (2003).
- [37] P. Sindzingre, G. Misguich, C. Lhuillier, B. Bernu, L. Pierre, Ch. Waldtmann, and H.-U. Everts Phys. Rev. Lett. **84**, 2953 (2000).
- [38] Jizhong Lou, Shaojin Qin, Tao Xiang, Changfeng Chen, Guang-Shan Tian, and Zhaobin Su, Phys. Rev. B **68**, 045110 (2003).
- [39] This case has been pointed by one the referee. I thank him/her for this remark.
- [40] D. C. Johnston, M. Troyer, S. Miyahara, D. Lidsky, K. Ueda, M. Azuma Z. Hiroi, M. Takano, M. Isobe, Y. Ueda, M. A. Korotin, V. I. Anisimov, A. V. Mahajan, L. L. Miller, cond-mat/0001147 (unpublished).
- [41] Eugene H. Kim, G. Fath, J. Solyom and D. J. Scalapino, Phys. Rev. B **62**, 14965 (2000).
- [42] Ningsheng Zhu, Xiaoqun Wang, Changfeng Chen, Phys. Rev. B **63**, 012401 (2001).
- [43] At 2nd order appears an additional contribution to the interchain interaction that could open a gap. However, this gap would be likely very small, probably much smaller than in the case of AF interchain coupling and difficult to see numerically.
- [44] O. A. Starykh, R. R. P. Singh, and G. C. Levine, Phys. Rev. Lett. **88**, 167203 (2002).